Published in final edited form as:
Sci Transl Med. 2012 April 25; 4(131): 131ra50. doi:10.1126/scitranslmed.3003623.

Suppression of Phosphoinositide 3-Kinase Signaling and Alteration of Multiple Ion Currents in Drug-Induced Long QT Syndrome

Zhongju Lu[1], **Chia-Yen C. Wu**[1], **Ya-Ping Jiang**[1], **Lisa M. Ballou**[1], **Chris Clausen**[1], **Ira S. Cohen**[1,*], and **Richard Z. Lin**[1,2,*]

[1]Department of Physiology and Biophysics and the Institute for Molecular Cardiology, Stony Brook University, Stony Brook, NY 11794, USA

[2]Northport Veterans Affairs Medical Center, Northport, NY 11768, USA

Abstract

Many drugs, including some commonly used medications, can cause abnormal heart rhythms and sudden death, as manifest by a prolonged QT interval in the electrocardiogram. Cardiac arrhythmias caused by drug-induced long QT syndrome are thought to result mainly from reductions in the delayed rectifier potassium ion (K^+) current I_{Kr}. Here, we report a mechanism for drug-induced QT prolongation that involves changes in multiple ion currents caused by a decrease in phosphoinositide 3-kinase (PI3K) signaling. Treatment of canine cardiac myocytes with inhibitors of tyrosine kinases or PI3Ks caused an increase in action potential duration that was reversed by intracellular infusion of phosphatidylinositol 3,4,5-trisphosphate. The inhibitors decreased the delayed rectifier K^+ currents I_{Kr} and I_{Ks}, the L-type calcium ion (Ca^{2+}) current $I_{Ca,L}$, and the peak sodium ion (Na^+) current I_{Na} and increased the persistent Na^+ current I_{NaP}. Computer modeling of the canine ventricular action potential showed that the drug-induced change in any one current accounted for less than 50% of the increase in action potential duration. Mouse hearts lacking the PI3K p110α catalytic subunit exhibited a prolonged action potential and QT interval that were at least partly a result of an increase in I_{NaP}. These results indicate that down-regulation of PI3K signaling directly or indirectly via tyrosine kinase inhibition prolongs the QT interval by affecting multiple ion channels. This mechanism may explain why some tyrosine kinase inhibitors in clinical use are associated with increased risk of life-threatening arrhythmias.

INTRODUCTION

Long QT syndrome is a disorder of the electrical activity of the heart that can lead to torsades de pointes arrhythmia and sudden death (1). As seen on an electrocardiogram (ECG), activation (depolarization) of the ventricle begins with the Q wave and the final repolarization of each beat occurs at the end of the T wave. Changes in ion fluxes that delay repolarization are detected clinically as an increase in the QT interval and can also be seen in vitro as an increase in the action potential duration (APD) in individual cardiac myocytes. Although understanding of the pathogenic mechanism is incomplete, it is thought that

*To whom correspondence should be addressed. ira.cohen@stonybrook.edu (I.S.C.); richard.lin@stonybrook.edu (R.Z.L.).

Competing interests: The authors declare that they have no competing interests.

Author contributions: Z.L., C.-Y.C.W., and Y.-P.J. performed the experiments and analyzed the data. C.C. and I.S.C. performed the computer simulation. L.M.B. contributed to the discussion, analyzed the data, and wrote the manuscript. R.Z.L. and I.S.C. supervised the study, analyzed the data, provided the funding, and wrote the manuscript.

excessive lengthening of the APD allows the L-type Ca^{2+} channel to recover from inactivation and initiate an early after-depolarization (EAD) whose probability of occurrence is enhanced by high sympathetic tone. Once produced, the EAD can be conducted slowly through the ventricle, leading to its reentry into regions already activated by the normal sinus beat, generating a macroscopic arrhythmia and possible sudden death.

Long QT syndrome can arise from congenital mutations that affect the function of individual ion channels that form the action potential or, in the acquired form, from drug inhibition of these channels. Most cases of congenital long QT syndrome are due to loss-of-function mutations in genes encoding the repolarizing K^+ channels that conduct the outward delayed rectifier currents I_{Kr} or I_{Ks} (1). Gain-of-function mutations in the gene encoding the depolarizing Na^+ channel that conducts the persistent Na^+ current (I_{NaP}) are found in a smaller number of patients (1). In addition, a mutation in ankyrin-B affecting multiple ion channels also leads to a long QT syndrome (2). Acquired long QT syndrome can be caused by many commonly used medications and limits the use of marketed drugs and the development of new drugs (3). Drugs that induce long QT syndrome are believed to almost invariably target I_{Kr}, and regulatory agencies recommend that all new drug candidates undergo in vitro testing for effects on I_{Kr} early in development (4). Drug binding to Kv11.1, the pore-forming subunit of the ion channel encoded by *KCNH2* (also called *hERG*), is the major mechanism for I_{Kr} inhibition (5, 6), although some drugs disrupt channel trafficking (7–9).

Tyrosine kinase inhibitors have recently entered clinical use as anti-cancer drugs (10, 11). Prescribing information for two of these drugs, dasatinib and sunitinib, warns that they can cause QT prolongation, and prescribing information for nilotinib contains a “black box” warning about the risk of QT prolongation and sudden death. Class IA phosphoinositide 3-kinases (PI3Ks), consisting of a catalytic subunit (p110α, p110β, or p110δ) bound to a p85 regulatory subunit, are activated by tyrosine kinases in many cell types by binding of Src homology 2 domains in p85 to tyrosine-phosphorylated proteins (12, 13). Here, we test the effects of dasatinib, sunitinib, and nilotinib on PI3K and APD in cardiac myocytes and the QT interval in isolated hearts to examine the mechanism by which these agents affect the QT interval.

RESULTS

APD prolongation induced by tyrosine kinase inhibitors is reversed by phosphatidylinositol 3,4,5-trisphosphate

The canine heart is the best-accepted animal model for the study of human cardiac electrophysiology (14). Canine ventricular myocytes are used by pharmaceutical companies and accepted by regulatory agencies as a screen for compounds for human use for the potential side effect of drug-induced long QT syndrome (15). The tyrosine kinase inhibitors nilotinib, dasatinib, and sunitinib cause long QT syndrome in humans. As expected, treatment of canine ventricular myocytes for 2 hours with these drugs induced a significant increase in APD_{90} (90% repolarization) (Fig. 1, A and B). Acute application of nilotinib for up to 5 min did not result in APD prolongation (fig. S1, A and C), indicating that the effect was most likely not a result of direct blockade of ion channels that determine the action potential. Two-hour treatment with the tyrosine kinase inhibitor imatinib, which does not cause long QT in humans, did not increase APD_{90} in canine myocytes (fig. S2A). The same concentration of drug completely blocked BCR-Abl autophosphorylation in human leukemia cells (fig. S2B), showing that Abl kinase was inhibited at this dose. To further demonstrate the usefulness of the canine model, treatment with terfenadine, the iconic long QT syndrome–inducing drug in humans, also pro-longed the APD_{90} in canine myocytes (fig. S3).

Because class IA PI3Ks can be activated by tyrosine kinases, we wondered whether suppression of PI3K activity by nilotinib, dasatinib, and sunitinib might contribute to the ability of these drugs to prolong the QT interval. First, we tested whether these tyrosine kinase inhibitors blocked serum activation of PI3K in isolated canine ventricular myocytes. Indeed, PI3K activity associated with tyrosine-phosphorylated proteins was substantially decreased in drug-treated myocytes compared to vehicle-treated cells (Fig. 1C). By contrast, imatinib did not cause a decrease in PI3K activity (fig. S2C). When phosphatidylinositol 3,4,5-trisphosphate (PIP_3), the second messenger produced by PI3K, was added to the patch pipette to dialyze the interior of cells treated with nilotinib, dasatinib, or sunitinib, the APD_{90} was shortened to control levels (Fig. 1, A and B). Intra-cellular infusion of control phospholipids phosphatidylinositol 3,5-bisphosphate [$PI(3,5)P_2$] or phosphatidylinositol 4,5-bisphosphate [$PI(4,5)P_2$] did not have this effect (Fig. 1B). These results indicate that inhibition of PI3K signaling is responsible for prolongation of the APD by these tyrosine kinase inhibitors that induce long QT syndrome in humans.

PI3K inhibitors induce APD prolongation and EADs

We next tested whether inhibitors that directly target PI3K also prolong the APD. Potent inhibitors of PI3K, such as BEZ235 (16), have already entered clinical trials for cancer therapy. We incubated canine myocytes for 2 hours with BEZ235 or with PI-103 (17), a chemically distinct PI3K inhibitor that is widely used in vitro, and both compounds significantly prolonged the APD_{90} (Fig. 2, A and B). The effect on APD was dose-dependent for both inhibitors, and BEZ235 had a smaller effect than PI-103 at each concentration (Fig. 2B). APD_{90} prolongation caused by PI3K inhibitors was larger than that caused by tyrosine kinase inhibitors. Infusion with PIP_3, but not $PI(4,5)P_2$ or $PI(3,5)P_2$, completely reversed the drug effects, confirming that the increase in APD was due to inhibition of PI3K (Fig. 2, A and B). As with nilotinib, acute application of PI-103 did not cause APD prolongation (fig. S1, B and C).

APD prolongation is associated with the development of EADs that may trigger arrhythmias. Because the probability of occurrence of EADs is enhanced by high sympathetic tone, we tested whether EADs are produced in myocytes exposed to PI3K inhibitors in the presence of isoproterenol (ISO). In canine myocytes exposed to ISO alone, there was a decrease in the plateau height and some APD shortening compared to untreated cells (fig. S4), but no EADs were induced in any of the control cells (0 of 10). In contrast, ISO induced EADs in the presence of 50 nM (8 of 10 cells) or 500 nM PI-103 (10 of 10 cells) (Fig. 2C). These data indicate that direct inhibition of PI3K might predispose to ventricular arrhythmias in the presence of increased sympathetic tone.

Multiple ion currents are affected by nilotinib and PI-103

Although nilotinib has been reported to reduce I_{Kr} (18), there is no a priori reason to assume that drug inhibition of PI3K signaling would affect only this current. We therefore looked for drug effects on other currents that regulate APD in canine myocytes treated with nilotinib or PI-103. Representative tracings (Fig. 3A) and current density–voltage (*I-V*) relationships (Fig. 3B) for the total time-dependent out-ward delayed rectifier current I_K show that the current density was smaller in cells incubated with nilotinib or PI-103 than in controls at test potentials greater than +10 mV. To discriminate between effects on the I_{Kr} or I_{Ks} component of I_K, we applied selective blockers of I_{Ks} (10 μM chromanol 293B) or I_{Kr} (1 μM dofetilide) to determine each current. The data show that the time-dependent chromanol-sensitive I_{Ks} density in nilotinib- or PI-103–treated cells was smaller than in controls at potentials greater than +10 mV, as was the time-dependent dofetilide-sensitive I_{Kr} density at all test potentials (Fig. 3, A and B).

Prolongation of the APD can also be caused by an increase in net inward currents during the action potential plateau. We therefore examined the inward Na^+ and Ca^{2+} currents in canine myocytes treated with nilotinib or PI-103. Representative tracings (Fig. 3C) and *I-V* relationships (Fig. 3D) show that both drugs increased the tetrodotoxin (TTX)–sensitive persistent Na^+ current I_{NaP} in 50 mM external Na^+ at all potentials tested. This concentration of external Na^+ was used because the magnitude of I_{NaP} is larger and thus the measurements more robust even though there can be escape from the membrane voltage clamp under these conditions. We also measured I_{NaP} with 10 mM external Na^+ when membrane voltage was well controlled and observed similar drug-induced increases in I_{NaP} (fig. S5, A and B). The peak Na^+ current I_{Na} was reduced by both nilotinib and PI-103 (fig. S5C). When normalized, the *I-V* relationships superimposed (fig. S5D), suggesting that the drugs cause a reduction in peak Na^+ conductance and indicating that I_{Na} was well clamped at 10 mM external Na^+. We previously reported that PI-103 causes a decrease in $I_{Ca,L}$ in canine myocytes (19). Nilotinib treatment also decreased $I_{Ca,L}$ at most of the potentials examined (fig. S6, A and B). These results show that direct inhibition of PI3K with PI-103 or indirect inhibition with nilotinib affects multiple ion channels that control the APD.

PIP_3 infusion or drug washout reverses the effect of nilotinib on I_{Kr} and I_{NaP}

We next investigated whether the effects of nilotinib on I_{Kr} and I_{NaP} are reversed after intracellular PIP_3 infusion or drug washout. In cells incubated with nilotinib, PIP_3 reversed the positive effect of the drug on I_{NaP} (Fig. 4, A and B) and the inhibitory effect of the drug on I_{Kr} (Fig. 4, C and D). Similarly, after the drug was washed away for 2 hours, both I_{NaP} (Fig. 4, A and B) and I_{Kr} (Fig. 4, C and D) returned to nearly control levels. However, both currents were still almost maximally affected after the drug was washed away for only 30 min (Fig. 4, A to D). Together with the PIP_3 infusion data and the lack of an acute effect of nilotinib on APD, the parsimonious explanation for the washout results is that these currents are regulated by PIP_3, which is slowly depleted after incubating myocytes with nilotinib and then gradually replenished after washing away the drug.

PI3K deletion increases I_{NaP} in mouse cardiac myocytes

Next, we used mouse strains lacking p110α or p110β in cardiac myocytes (19) to test the effect of decreased PI3K signaling on ion currents and the action potential without using pharmacological inhibitors. We reported previously that $I_{Ca,L}$ in mouse cardiac myocytes is inhibited by deletion of p110α but not p110β (19). Delayed rectifier currents in mouse myocytes are very small and are thought to contribute little to the mouse APD, so they are not considered here. We therefore tested whether the sodium currents affected by nilotinib and PI-103 in dog myocytes are similarly affected by p110α ablation in the mouse. As in canine cells, I_{NaP} was markedly enhanced in p110α-null mouse myocytes when measured with either 50 mM (Fig. 5, A and B) or 10 mM (fig. S7, A and B) external Na^+. I_{Na} was also reduced in $p110\alpha^{-/-}$ myocytes compared to wild-type myocytes (fig. S7C). When normalized, the I_{Na}-*V* relationships superimposed (fig. S7D), indicating that I_{Na} was well clamped at 10 mM external Na^+. In contrast, ablation of p110β did not affect I_{NaP} or I_{Na} (Fig. 5 and fig. S7).

Decreased PI3K signaling causes increased APD and QT prolongation in the mouse

We also tested whether decreased PI3K signaling leads to prolongation of the APD in the mouse. Mouse APD was measured in the presence of 4-aminopyridine (4-AP) to reduce the large transient outward K^+ current that allows the rapid heart rate in this species. Under these conditions, APD_{90} in $p110\alpha^{-/-}$ myocytes was markedly longer than in wild-type cells, and APD_{90} in wild-type cells treated with PI-103 was almost as long as in $p110\alpha^{-/-}$ myocytes (Fig. 6, A and B). Treatment of $p110\alpha^{-/-}$ myocytes with a p110β-specific inhibitor (TGX-221) or nilotinib did not further prolong the APD_{90}, but, as expected,

intracellular dialysis of PIP_3 shortened the APD (Fig. 6B). In contrast, ablation of p110β had minimal effects on the APD_{90}, and treatment of p110β $^{-/-}$ myocytes with a p110α-specific inhibitor (PIK-75) lengthened the APD_{90} to nearly the level observed in p110α$^{-/-}$ myocytes (Fig. 6B). Together, these results indicate that p110α rather than p110β is the dominant PI3K that regulates the APD in mouse myocytes and suggest that APD prolongation induced by nilotinib, PI-103, or p110α ablation is mediated by the common mechanism of reduced PI3K signaling.

To determine whether p110α ablation results in prolongation of the QT interval, we recorded ECGs from isolated hearts. The QT interval corrected for heart rate (QTc) was almost twice as long in p110α$^{-/-}$ hearts (60 ms) than in wild-type hearts (31 ms) (Fig. 6, C and D). Nilotinib increased the QTc of wild-type hearts but did not have an additional effect on p110α$^{-/-}$ hearts (Fig. 6, C and D). Last, we confirmed that PI-103 also increased QTc in wild-type hearts (Fig. 6, C and D).

Alterations in multiple ion currents account for APD prolongation caused by nilotinib and PI-103

Nilotinib and PI-103 affected multiple ion channels that could exert opposing effects on the APD. The decrease in I_{Kr} and I_{Ks} and increase in I_{NaP} could lengthen the APD, whereas inhibition of $I_{Ca,L}$ and I_{Na} could shorten the APD. To determine the theoretical impact of the sum total of these current changes on the action potential, we used a modified Hund-Rudy model of the canine ventricular action potential (20). Figure 7A shows the fractional change in each current that we measured in cells treated with nilotinib or PI-103, and Fig. 7B shows the action potentials generated by the computer simulation incorporating these changes. The control action potential generated an APD_{90} of 216 ms, whereas the APD_{90} with nilotinib or PI-103 was 343 or 323 ms, respectively. These results agree with the experimental data showing that these compounds produce a lengthening of the APD. Although nilotinib and PI-103 affected multiple channels, it was still possible that most of the effect on APD prolongation was due to the 60% reduction in I_{Kr} and that the long QT syndrome induced by inhibition of PI3K would still be predominantly an I_{Kr} disease. Also shown in Fig. 7 is the result of a simulation in which the only parameter change was a reduction in I_{Kr} to 40% of control (ΔI_{Kr}), which generated an APD_{90} of 256 ms. Thus, less than half of the change in APD_{90} induced by either drug is due to the reduction in I_{Kr}. Similarly, the APD_{90}s generated from single-parameter changes in the other currents (ΔI_{Ks}, ΔI_{NaP}, etc.) were all less than 256 ms (Fig. 7A). On the other hand, mathematical modeling showed that alterations in just I_{Kr} and I_{NaP} account for about 80% of APD_{90} prolongation due to PI3K inhibition in canine myocytes (Fig. 7B). These simulations indicate that inhibition of PI3K lengthens the APD by affecting multiple ion currents, especially I_{Kr} plus I_{NaP}, and not an individual current. These results are consistent with a report in which Noble's group used computer modeling to illustrate how alterations in multiple ion currents by drugs could be a better predictor of long QT–induced arrhythmias than inhibition only of I_{Kr} (21).

Suppression of I_{NaP} ameliorates the QT prolongation by PI3K inhibition

We next sought to confirm experimentally that the increase in I_{NaP} caused by PI3K inhibition contributes to APD prolongation and EAD generation in canine myocytes. Cells were treated with BEZ235 in the presence or absence of mexiletine, a relatively selective I_{NaP} inhibitor. Mexiletine caused a small decrease in APD_{90} in control cells, but it reduced the APD_{90} in BEZ235-treated myocytes from 450 ms to about 300 ms (Fig. 8, A and B). These data support the conclusion of the computer simulations that an increase in I_{NaP} plays animportantrole indrug-induced APD prolongation. Mexiletine also prevented EADs in canine myocytes treated with BEZ235. ISO stimulation of BEZ235-treated cells induced EADs in 10 of 10 myocytes (Fig. 8, C and D). When the cells were treated with mexiletine

in conjunction with BEZ235, ISO stimulation induced EADs in only 1 of 10 of the myocytes (Fig. 8D). These results suggest that selective blockers of I_{NaP} could be used to counter-act drug-induced long QT syndrome involving the PI3K signaling pathway.

We also tested whether the increase in I_{NaP} contributes to QTc prolongation in p110α$^{-/-}$ hearts. We found that mexiletine markedly reduced the QTc interval in p110α$^{-/-}$ hearts but had no effect on QTc in wild-type hearts (Fig. 8, E and F). These results indicate that an increase in I_{NaP} also plays a role in the long QT phenotype caused by down-regulation of PI3K signaling in the mouse heart.

DISCUSSION

Reports in the 1980s and 1990s that Seldane (terfenadine), the first antihistamine free of soporific side effects, induced life-threatening arrhythmias associated with sudden death markedly changed how the pharmaceutical industry tests candidate drugs to meet Food and Drug Administration safety requirements (22). The prevailing view regarding drug-induced long QT syndrome has been that it is mainly an I_{Kr} disease resulting from direct blockade of the Kv11.1 ion channel by pharmaceutical agents (3). Our study introduces an alternative view for the basis of drug-induced long QT syndrome. We show that inhibition of PI3K signaling can be arrhythmogenic and is the major cause of nilotinib-induced action potential prolongation. Decreased PI3K signaling affects multiple currents in cardiac myocytes, and this complex alteration of both inward and outward ionic fluxes leads to prolongation of the action potential and the QT interval.

Acute treatment of rodent cardiac my-ocytes with the PI3K inhibitor LY294002 caused APD prolongation and EADs (23, 24). These effects were attributed to direct inhibition of outward K^+ currents by LY294002 rather than inhibition of PI3K. In contrast, we found that APD prolongation in canine myocytes was elicited only after prolonged exposure to inhibitors of tyrosine kinases or PI3K. The slow reversal of the effects of nilotinib on I_{Kr} and I_{NaP} after drug washout, together with the rapid PIP_3-induced reversal of the effects of inhibitors, supports our conclusion that PI3K inhibition underlies the effects of these drugs.

Some studies have examined modulation of individual ion channels relevant to this work by PI3K and its downstream effector, the protein kinase Akt. Kv11.1 expressed in human embryonic kidney (HEK) 293 cells was highly phosphorylated (25). Zhang *et al.* (26) showed that PI3K/Akt signaling in HEK293 cells maintained the Kv11.1-induced current, and expression of constitutively active forms of PI3K p110α or Akt caused an increase in current density. These investigators speculated that Akt might regulate the current by modifying consensus Akt phosphorylation sites identified in Kv11.1 (26). We showed that PI3K/Akt inhibition decreases $I_{Ca,L}$ by reducing the number of channels on the myocyte surface (19), and Viard *et al.* (27) demonstrated that Ca^{2+} channel trafficking to the cell surface is enhanced by Akt-dependent phosphorylation. I_{Ks} is also modulated by trafficking (28). The increase in I_{NaP} after PI3K inhibition is probably not due to trafficking of Nav1.5 sodium channels to the plasma membrane because peak I_{Na} was concomitantly decreased. Instead, it is more likely due to an increase in open probability of the persistent gating state. One potential mechanism to induce such a gating change is phosphorylation of Akt consensus sites in Nav1.5.

Because of electrophysiological differences between species, mouse models of congenital K^+ channel long QT syndromes in general have not been highly informative with regard to the human diseases. On the other hand, mouse models of sodium channel mutations that cause an increase in I_{NaP} exhibit most of the phenotypes seen in patients with type 3 congenital long QT syndrome (LQT3) who have gain-of-function mutations in Nav1.5

(encoded by *SCN5A*) (29, 30). Expression of two different *SCN5A* mutants found in human LQT3 led to an increase in I_{NaP}, significant prolongation of the QT interval, and development of cardiac arrhythmias in mice (31, 32). Mexiletine treatment reversed the APD prolongation in myocytes expressing a Nav1.5 mutant but did not affect APD in myocytes from wild-type mice (32). Our finding that mexiletine shortened QTc in p110α-null hearts but not in wild-type hearts is consistent with a prominent role of PI3K in regulating I_{NaP}.

Mexiletine shortens QTc in LQT3 patients (33). Our results suggest that mexiletine may serve as a useful adjuvant to ameliorate some of the APD lengthening and EADs induced by inhibition of PI3K. The use of β-adrenergic receptor blockers to reduce the probability of EAD initiation could have serious side effects on contractility because PI3K inhibition already induces a significant reduction in $I_{Ca,L}$. However, reduction of $I_{Ca,L}$ probably has an anti–long QT effect, because it tends to shorten the APD.

The incidence of QT prolongation in patients taking nilotinib was reported to be 1 to 10% (34). Cancer patients often have multiple risk factors, such as electrolyte disturbances, heart disease, and use of other medications that prolong the QT interval that might make them especially vulnerable to long QT syndrome induced by tyrosine kinase or PI3K inhibitors. Our results suggest that patients treated with tyrosine kinase inhibitors, PI3K inhibitors, or other drugs that target PI3K signaling in the heart should be closely monitored for QT prolongation and cardiac arrhythmias. Some tyrosine kinase inhibitors such as imatinib might be innocuous because the enzymes they target do not regulate cardiac PI3K.

Our results suggest that known long QT syndrome–inducing drugs should be reinvestigated to determine whether they affect PI3K signaling. Indeed, we found that infusion with PIP_3 reversed the terfenadine-induced APD prolongation by ~80% (fig. S3). Furthermore, terfenadine increased I_{NaP}, and this effect on the sodium current was completely reversed by PIP_3 infusion (fig. S8). These results suggest that this iconic long QT syndrome–inducing drug not only directly blocks I_{Kr} but also affects the PI3K signaling pathway to prolong the QT interval.

Patients receiving 400 mg of nilotinib twice daily exhibited mean peak and trough serum concentrations of 3.6 and 1.7 μM, respectively (35). Patients taking 1600 mg of BEZ235 per day had a maximal median steady-state serum concentration of 3.8 μM (36). Although some of the compounds we tested might directly block ion channels at higher pharmacological concentrations, our results indicate that inhibition of PI3K is the dominant factor that causes APD prolongation. However, when considering the role PI3K plays in drug-induced long QT syndrome, it is important to realize the limitations in applying our results to testing of new compounds during drug development. First, like all studies of this kind, results were obtained from animal models, which might not translate to the human condition when dealing with new compounds. Second, to make a definitive statement concerning the safety of a drug candidate, it is necessary to know the therapeutic concentration of drug candidate compared to the dose-response curves for PI3K inhibition and direct channel blockade. Nevertheless, our results may necessitate changes in the safety testing requirements for new drugs and indicate that drugs in clinical use that inhibit PI3K signaling could pose significant cardiac risks.

MATERIALS AND METHODS

Animals

Mixed-breed dogs of either sex more than 12 months old were purchased from R&R Research. The MerCreMer;$p110\alpha^{Flox/Flox}$ and MerCreMer; $p110\beta^{Flox/Flox}$ mouse models

were described earlier (19). At 8 to 9 weeks of age, mice were injected intraperitoneally with 1 mg of tamoxifen (Sigma) five times a week for 4 weeks to knock out the *Pik3ca* or *Pik3cb* gene, and the animals were analyzed at 5 to 6 months of age. All animal-related experimental protocols were approved by the Stony Brook University Institutional Animal Care and Use Committee.

Ventricular myocyte isolation

Canine ventricular cells were isolated from the mid-myocardium as described (19). Mouse ventricular myocytes were isolated as described (37).

Electrophysiology

Isolated myocytes were stored in KB (Kraftbrühe) solution and then placed in a temperature-controlled chamber. Recordings were made at room temperature unless otherwise indicated. Only relaxed quiescent cells displaying clear cross striations were used. Standard whole-cell patch-clamp techniques were performed with an Axopatch-1D amplifier with a CV-4 1/100 headstage (Axon Instruments). A PC equipped with 12-bit AD/DA converters (model 1360, Cambridge Electronic Design) was used for data acquisition, generation of pulse protocols, and data analysis. Currents were filtered with a four-pole Bessel filter at 2 kHz and digitized at 1 kHz. Current amplitude was normalized to cell capacitance to obtain current density. Pipette and external solutions are described in the Supplementary Materials. In some experiments, 1 μM phospholipids (all di-C8, Echelon Biosciences) were added to the pipette solution. Chromanol 293B, dofetilide, 4-AP, and ISO were obtained from Sigma and were freshly prepared before experiments. Dasatinib monohydrate (ChemieTek), nilotinib (ChemieTek), sunitinib malate (LC Laboratories), imatinib mesylate (Selleckchem), terfenadine (Sigma), mexiletine hydrochloride (Sigma), PI-103 (Cayman Chemical), or BEZ235 (Cayman Chemical) was added to cells for 2 hours at room temperature before patch clamping, except where otherwise noted.

Recording of action potentials in canine myocytes was initiated in current clamp mode by applying a 180-pA depolarizing stimulus for 15 ms with cycle lengths from 1 to 3 s. The pulses were 120 pA in amplitude and 10 ms in duration for mouse myocytes with a cycle length of 1 s. The APD was determined at 90% repolarization. At least 10 consecutive stable action potentials were recorded within 5 min after going into whole-cell configuration. A sufficient number of stimuli were applied at each frequency before measurements were taken so that the APD was at steady state. Because of the shorter APD in mouse than in canine ventricular myocytes, mainly caused by a larger transient outward current I_{to}, minor changes in APD caused by drugs may be missed or underestimated. Thus, 2 mM 4-AP was added to the external solution for mouse myocytes to block most of the transient outward current and prolong the APD for easier comparison to the canine APD (38).

I_K was generated by 5-s depolarizing test voltage pulses ranging from −20 to 60 mV in 10-mV increments and then returned to −20 mV for 5 s. The pulse frequency was 0.05 Hz and the holding potential was −40 mV to inactivate Na^+ current. Typically, total I_K was measured first. Then, the cell was exposed to chromanol 293B (10 μM, Sigma), and I_{Ks} was determined by subtracting I_K plus chromanol 293B from total I_K. Further addition of dofetilide (1 μM, Sigma) to the same cell allowed I_{Kr} to be determined by subtracting the current traces in the presence of chromanol 293B plus dofetilide from those in the presence of chromanol 293B. For the reversal experiments where only I_{Kr} was measured, dofetilide was added alone. The amplitudes of I_K, I_{Kr}, and I_{Ks} were measured as the difference between the instantaneous current immediately after the application of the depolarizing voltage step and the current level at the end of the test pulse. Ca^{2+} current and I_{to} were inhibited by including $CdCl_2$ and 4-AP, respectively, in the external solution.

The TTX-sensitive Na^+ current was elicited by 750-ms depolarizing voltage steps ranging from −80 to +50 mV at 10-mV increments from a holding potential of −80 mV. I_{Na} was measured as the peak negative current, and I_{NaP} was measured as the main inward current between 700 and 750 ms at the end of depolarization. TTX-sensitive currents were measured by subtracting a trace obtained in the presence of 10 μM TTX from a trace obtained in the absence of TTX. I_{NaP} records were filtered at 20 Hz. For the single trace of TTX-sensitive current shown in the figures, the current was activated at a test voltage of −20 mV from a holding potential of −80 mV.

Recording of $I_{Ca,L}$ was performed as described (19).

ECG recordings from mouse hearts ex vivo

Isolated mouse hearts were mounted on the Harvard Apparatus isolated heart perfusion system (IH-SR) and perfused with Krebs-Henseleit solution (118 mM NaCl, 4.7 mM KCl, 2.52 mM $CaCl_2$, 1.64 mM $MgSO_4$, 24.88 mM $NaHCO_3$, 1.18 mM KH_2PO_4, 5.55 mM glucose, and 2 mM sodium pyruvate aerated with 5% CO_2 and 95% O_2) at 37°C for 30 min to reach a stable baseline before data collection. For ECG recording, we placed one electrode at the base of the heart next to the left atrium and a second electrode at the heart apex. Recordings were collected under control conditions, and then drugs were added to the perfusate reservoir and circulated through the system for 30 min before collecting another set of ECG recordings. QT intervals were measured automatically by the LabChart 7.1.2 (ADInstruments) software system from >30 consecutive heartbeats, and QTc was calculated with the correction described by Mitchell *et al.* (39).

PI3K activity

Lysates prepared from canine myocytes were immunoprecipitated with an anti-phosphotyrosine antibody (Millipore) and then subjected to PI3K activity assays as described (40).

Computer simulation of canine action potential

A modified version (41) of the Hund-Rudy mathematical model (20) that describes action potentials in isolated ventricular myocytes was used in computer simulations. Computing was performed in the MATLAB computing environment. The model was integrated with library routine ode15s, an adaptive algorithm that adjusts integration time increments to maintain a relative tolerance of better than 10^{-3}, or an absolute tolerance of better than 10^{-6}. In all cases, the model was paced at 1 Hz to a steady state. I_K, I_{Ks}, and I_{Kr} were measured at a test voltage of +60 mV from a holding potential of −40 mV. I_{NaP} and I_{Na} were measured at test voltages of −40 and 0 mV, respectively. The holding potential was −80 mV. $I_{Ca,L}$ was measured at a test voltage of +10 mV from a holding potential of −50 mV. All currents were normalized to cell capacitance. In all cases, we assumed a change in conductance that is not voltage-dependent for this initial computation. This assumption is roughly valid for all but I_{Ks}, which is affected only at positive potentials but has only a small effect on the computed APD by itself.

Supplementary Material

Refer to Web version on PubMed Central for supplementary material.

Acknowledgments

We thank J. Zuckerman for preparing the cardiac myocytes and M. Rosen for his helpful discussion.

Funding: This work was funded by NIH grants DK62722 (R.Z.L.), HL67101 (I.S.C.), and HL94410 (I.S.C.); a Veterans Affairs Merit Award (R.Z.L.); and grants from the American Diabetes Association (R.Z.L.) and the Juvenile Diabetes Research Foundation (R.Z.L.).

REFERENCES AND NOTES

1. Hedley PL, Jørgensen P, Schlamowitz S, Wangari R, Moolman-Smook J, Brink PA, Kanters JK, Corfield VA, Christiansen M. The genetic basis of long QT and short QT syndromes: A mutation update. Hum Mutat. 2009; 30:1486–1511. [PubMed: 19862833]
2. Mohler PJ, Schott JJ, Gramolini AO, Dilly KW, Guatimosim S, duBell WH, Song LS, Haurogné K, Kyndt F, Ali ME, Rogers TB, Lederer WJ, Escande D, Le Marec H, Bennett V. Ankyrin-B mutation causes type 4 long-QT cardiac arrhythmia and sudden cardiac death. Nature. 2003; 421:634–639. [PubMed: 12571597]
3. Roden DM. Drug-induced prolongation of the QT interval. N Engl J Med. 2004; 350:1013–1022. [PubMed: 14999113]
4. The Non-Clinical Evaluation of the Potential for Delayed Ventricular Repolarization (QT Interval Prolongation) by Human Pharmaceuticals. International Conference on Harmonisation of Technical Requirements for Registration of Pharmaceuticals for Human Use; Geneva. 2005.
5. Mitcheson JS. hERG potassium channels and the structural basis of drug-induced arrhythmias. Chem Res Toxicol. 2008; 21:1005–1010. [PubMed: 18447395]
6. Mitcheson JS, Chen J, Sanguinetti MC. Trapping of a methanesulfonanilide by closure of the HERG potassium channel activation gate. J Gen Physiol. 2000; 115:229–240. [PubMed: 10694252]
7. Ficker E, Kuryshev YA, Dennis AT, Obejero-Paz C, Wang L, Hawryluk P, Wible BA, Brown AM. Mechanisms of arsenic-induced prolongation of cardiac repolarization. Mol Pharmacol. 2004; 66:33–44. [PubMed: 15213294]
8. Kuryshev YA, Ficker E, Wang L, Hawryluk P, Dennis AT, Wible BA, Brown AM, Kang J, Chen XL, Sawamura K, Reynolds W, Rampe D. Pentamidine-induced long QT syndrome and block of hERG trafficking. J Pharmacol Exp Ther. 2005; 312:316–323. [PubMed: 15340016]
9. Dennis A, Wang L, Wan X, Ficker E. hERG channel trafficking: Novel targets in drug-induced long QT syndrome. Biochem Soc Trans. 2007; 35:1060–1063. [PubMed: 17956279]
10. Agrawal M, Garg RJ, Cortes J, Quintás-Cardama A. Tyrosine kinase inhibitors: The first decade. Curr Hematol Malig Rep. 2010; 5:70–80. [PubMed: 20425399]
11. Adams VR, Leggas M. Sunitinib malate for the treatment of metastatic renal cell carcinoma and gastrointestinal stromal tumors. Clin Ther. 2007; 29:1338–1353. [PubMed: 17825686]
12. Backer JM, Myers MG Jr, Shoelson SE, Chin DJ, Sun XJ, Miralpeix M, Hu P, Margolis B, Skolnik EY, Schlessinger J, White MF. Phosphatidylinositol 3′-kinase is activated by association with IRS-1 during insulin stimulation. EMBO J. 1992; 11:3469–3479. [PubMed: 1380456]
13. Carpenter CL, Auger KR, Chanudhuri M, Yoakim M, Schaffhausen B, Shoelson S, Cantley LC. Phosphoinositide 3-kinase is activated by phosphopeptides that bind to the SH2 domains of the 85-kDa subunit. J Biol Chem. 1993; 268:9478–9483. [PubMed: 7683653]
14. Skadsberg, ND.; Hill, AJ.; Iaizzo, PA. Isolated heart models. In: Sigg, DC.; Iaizzo, PA.; Xiao, Y-F.; He, B., editors. Cardiac Electrophysiology Methods and Models. Springer; New York: 2010. p. 249-260.
15. Redfern WS, Carlsson L, Davis AS, Lynch WG, MacKenzie I, Palethorpe S, Siegl PK, Strang I, Sullivan AT, Wallis R, Camm AJ, Hammond TG. Relationships between preclinical cardiac electrophysiology, clinical QT interval prolongation and torsade de pointes for a broad range of drugs: Evidence for a provisional safety margin in drug development. Cardiovasc Res. 2003; 58:32–45. [PubMed: 12667944]
16. Maira SM, Stauffer F, Brueggen J, Furet P, Schnell C, Fritsch C, Brachmann S, Chene P, De Pover A, Schoemaker K, Fabbro D, Gabriel D, Simonen M, Murphy L, Finan P, Sellers W, Garcia-Echeverria C. Identification and characterization of NVP-BEZ235, a new orally available dual phosphatidylinositol 3-kinase/mammalian target of rapamycin inhibitor with potent in vivo antitumor activity. Mol Cancer Ther. 2008; 7:1851–1863. [PubMed: 18606717]
17. Raynaud FI, Eccles S, Clarke PA, Hayes A, Nutley B, Alix S, Henley A, Di-Stefano F, Ahmad Z, Guillard S, Bjerke LM, Kelland L, Valenti M, Patterson L, Gowan S, de Haven Brandon A,

Hayakawa M, Kaizawa H, Koizumi T, Ohishi T, Patel S, Saghir N, Parker P, Waterfield M, Workman P. Pharmacologic characterization of a potent inhibitor of class I phosphatidylinositide 3-kinases. Cancer Res. 2007; 67:5840–5850. [PubMed: 17575152]

18. Freebern WJ, Fang HS, Slade MD, Wells S, Canale J, Megill J, Grubor B, Shi H, Fletcher A, Lombardo L, Levesque P, Lee FY, Sasseville VG. In vitro cardiotoxicity potential comparative assessments of chronic myelogenous leukemia tyrosine kinase inhibitor therapies: Dasatinib, imatinib and nilotinib. Blood. 2007; 110:abstract 4582.
19. Lu Z, Jiang YP, Wang W, Xu XH, Mathias RT, Entcheva E, Ballou LM, Cohen IS, Lin RZ. Loss of cardiac phosphoinositide 3-kinase p110α results in contractile dysfunction. Circulation. 2009; 120:318–325. [PubMed: 19597047]
20. Hund TJ, Rudy Y. Rate dependence and regulation of action potential and calcium transient in a canine cardiac ventricular cell model. Circulation. 2004; 110:3168–3174. [PubMed: 15505083]
21. Mirams GR, Cui Y, Sher A, Fink M, Cooper J, Heath BM, McMahon NC, Gavaghan DJ, Noble D. Simulation of multiple ion channel block provides improved early prediction of compounds' clinical torsadogenic risk. Cardiovasc Res. 2011; 91:53–61. [PubMed: 21300721]
22. Monahan BP, Ferguson CL, Killeavy ES, Lloyd BK, Troy J, Cantilena LR Jr. Torsades de pointes occurring in association with terfenadine use. JAMA. 1990; 264:2788–2790. [PubMed: 1977935]
23. Sun H, Oudit GY, Ramirez RJ, Costantini D, Backx PH. The phosphoinositide 3-kinase inhibitor LY294002 enhances cardiac myocyte contractility via a direct inhibition of $I_{k,\,slow}$ currents. Cardiovasc Res. 2004; 62:509–520. [PubMed: 15158143]
24. Oudit GY, Sun H, Kerfant BG, Crackower MA, Penninger JM, Backx PH. The role of phosphoinositide-3 kinase and PTEN in cardiovascular physiology and disease. J Mol Cell Cardiol. 2004; 37:449–471. [PubMed: 15276015]
25. Cockerill SL, Tobin AB, Torrecilla I, Willars GB, Standen NB, Mitcheson JS. Modulation of hERG potassium currents in HEK-293 cells by protein kinase C. Evidence for direct phosphorylation of pore forming subunits. J Physiol. 2007; 581:479–493. [PubMed: 17363390]
26. Zhang Y, Wang H, Wang J, Han H, Nattel S, Wang Z. Normal function of HERG K+ channels expressed in HEK293 cells requires basal protein kinase B activity. FEBS Lett. 2003; 534:125–132. [PubMed: 12527373]
27. Viard P, Butcher AJ, Halet G, Davies A, Nurnberg B, Heblich F, Dolphin AC. PI3K promotes voltage-dependent calcium channel trafficking to the plasma membrane. Nat Neurosci. 2004; 7:939–946. [PubMed: 15311280]
28. Strutz-Seebohm N, Henrion U, Steinke K, Tapken D, Lang F, Seebohm G. Serum- and glucocorticoid-inducible kinases (SGK) regulate KCNQ1/KCNE potassium channels. Channels. 2009; 3:88–90. [PubMed: 19372749]
29. Salama G, London B. Mouse models of long QT syndrome. J Physiol. 2007; 578:43–53. [PubMed: 17038432]
30. Charpentier F, Bourgé A, Mérot J. Mouse models of *SCN5A*-related cardiac arrhythmias. Prog Biophys Mol Biol. 2008; 98:230–237. [PubMed: 19041666]
31. Nuyens D, Stengl M, Dugarmaa S, Rossenbacker T, Compernolle V, Rudy Y, Smits JF, Flameng W, Clancy CE, Moons L, Vos MA, Dewerchin M, Benndorf K, Collen D, Carmeliet E, Carmeliet P. Abrupt rate accelerations or premature beats cause life-threatening arrhythmias in mice with long-QT3 syndrome. Nat Med. 2001; 7:1021–1027. [PubMed: 11533705]
32. Tian XL, Yong SL, Wan X, Wu L, Chung MK, Tchou PJ, Rosenbaum DS, Van Wagoner DR, Kirsch GE, Wang Q. Mechanisms by which *SCN5A* mutation N1325S causes cardiac arrhythmias and sudden death in vivo. Cardiovasc Res. 2004; 61:256–267. [PubMed: 14736542]
33. Schwartz PJ, Priori SG, Locati EH, Napolitano C, Cantù F, Towbin JA, Keating MT, Hammoude H, Brown AM, Chen LS. Long QT syndrome patients with mutations of the *SCN5A* and *HERG* genes have differential responses to Na+ channel blockade and to increases in heart rate. Implications for gene-specific therapy. Circulation. 1995; 92:3381–3386. [PubMed: 8521555]
34. Yeh ET, Bickford CL. Cardiovascular complications of cancer therapy: Incidence, pathogenesis, diagnosis, and management. J Am Coll Cardiol. 2009; 53:2231–2247. [PubMed: 19520246]
35. Kantarjian H, Giles F, Wunderle L, Bhalla K, O'Brien S, Wassmann B, Tanaka C, Manley P, Rae P, Mietlowski W, Bochinski K, Hochhaus A, Griffin JD, Hoelzer D, Albitar M, Dugan M, Cortes

J, Alland L, Ottmann OG. Nilotinib in imatinib-resistant CML and Philadelphia chromosome–positive ALL. N Engl J Med. 2006; 354:2542–2551. [PubMed: 16775235]

36. Peyton JD, Rodon Ahnert J, Burris H, Britten C, Chen LC, Tabernero J, Duval V, Rouyrre N, Silva A, Quadt C, Baselga J. A dose-escalation study with the novel formulation of the oral pan-class I PI3K inhibitor BEZ235, solid dispersion system (SDS) sachet, in patients with advanced solid tumors. J Clin Oncol. May 20.2011 29(Supplement):abstract 3066.
37. Fan G, Jiang YP, Lu Z, Martin DW, Kelly DJ, Zuckerman JM, Ballou LM, Cohen IS, Lin RZ. A transgenic mouse model of heart failure using inducible Gαq. J Biol Chem. 2005; 280:40337–40346. [PubMed: 16210321]
38. Wang L, Duff HJ. Developmental changes in transient outward current in mouse ventricle. Circ Res. 1997; 81:120–127. [PubMed: 9201035]
39. Mitchell GF, Jeron A, Koren G. Measurement of heart rate and Q-T interval in the conscious mouse. Am J Physiol. 1998; 274:H747–H751. [PubMed: 9530184]
40. Ballou LM, Cross ME, Huang S, McReynolds EM, Zhang BX, Lin RZ. Differential regulation of the phosphatidylinositol 3-kinase/Akt and p70 S6 kinase pathways by the α1A-adrenergic receptor in rat-1 fibroblasts. J Biol Chem. 2000; 275:4803–4809. [PubMed: 10671514]
41. Lau DH, Clausen C, Sosunov EA, Shlapakova IN, Anyukhovsky EP, Danilo P Jr, Rosen TS, Kelly C, Duffy HS, Szabolcs MJ, Chen M, Robinson RB, Lu J, Kumari S, Cohen IS, Rosen MR. Epicardial border zone overexpression of skeletal muscle sodium channel SkM1 normalizes activation, preserves conduction, and suppresses ventricular arrhythmia: An in silico, in vivo, in vitro study. Circulation. 2009; 119:19–27. [PubMed: 19103989]

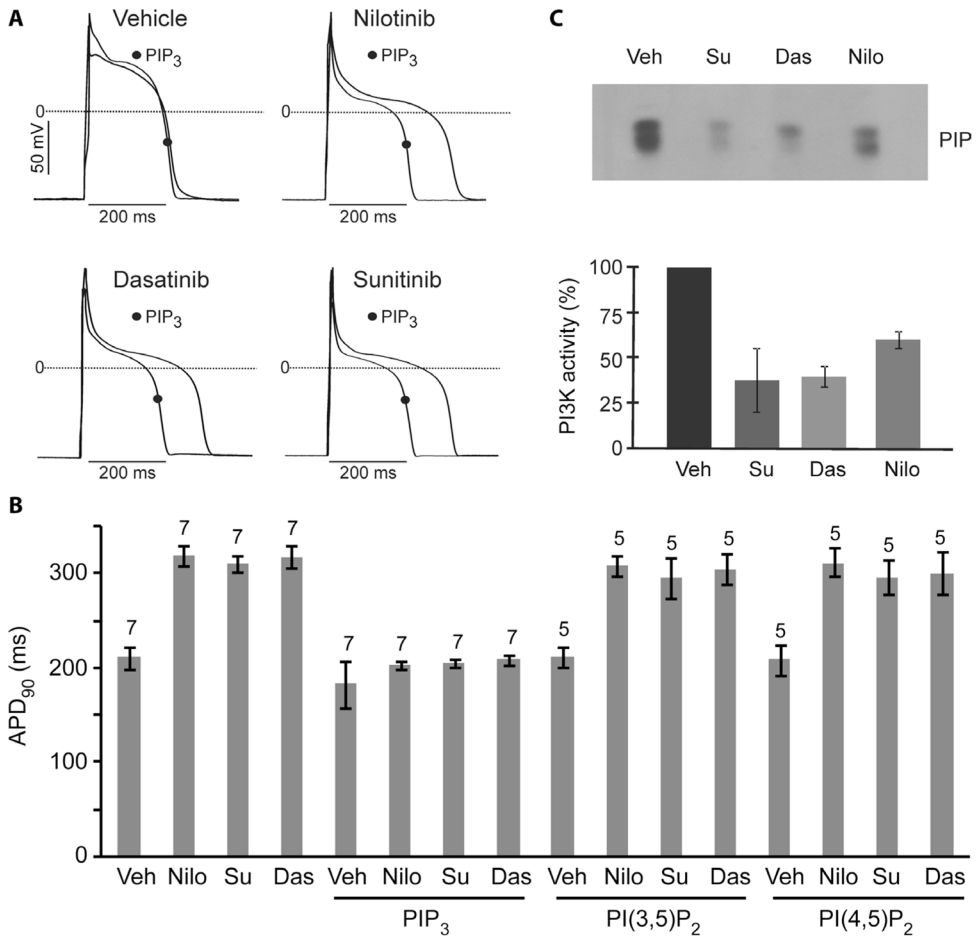

Fig. 1.

Prolonged APD caused by tyrosine kinase inhibitors in canine myocytes and reversal by PIP_3 infusion. (**A**) Sample traces of action potentials in myocytes treated with vehicle or drugs (1 μM for 2 hours) with or without intracellular infusion of 1 μM PIP_3. (**B**) Summary data of APD_{90} in myocytes treated with tyrosine kinase inhibitors with or without infusion of 1 μM phospholipids. Data are means ± SE. The number of cells studied is above each bar. (**C**) Myocytes were treated with vehicle (Veh) or dasatinib (Das), nilotinib (Nilo), or sunitinib (Su) at 1 μM for 1 hour and then stimulated with 7.5% fetal bovine serum for 5 min. PI3K activity was assayed in anti-phosphotyrosine immunoprecipitates of cell lysates. The upper panel is an autoradiograph from a representative assay showing [^{32}P]phosphatidylinositol 3-phosphate (PIP), and the lower graph summarizes data from three independent experiments. Data are means ± SE.

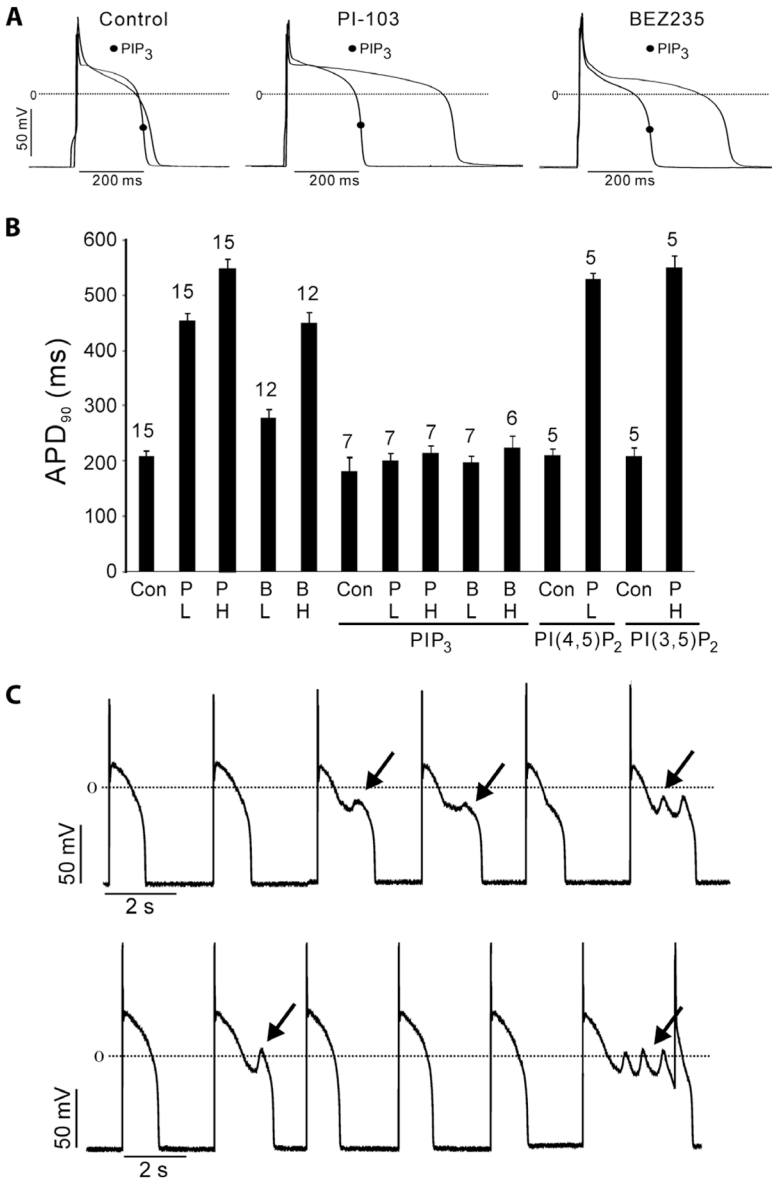

Fig. 2.

Prolonged APD and EADs caused by PI3K inhibitors in canine myocytes. (**A**) Sample traces of action potentials in myocytes treated with inhibitor (500 nM for 2 hours) or left untreated as control with or without intracellular infusion of 1 μM PIP_3. (**B**) Summary data of APD_{90} in myocytes treated with 50 nM (L) or 500 nM (H) PI-103 (P) or BEZ235 (B) with or without infusion of 1 μM phospholipids. Data are means ± SE. The number of cells studied is above each bar. (**C**) ISO (5 μM)–induced EADs (arrows) in myocytes treated with 50 nM (upper panel) or 500 nM (lower panel) PI-103. Action potentials were initiated in current clamp mode by applying a 180-pA depolarizing stimulus for 15 ms at a cycle length of 3 s and were recorded at 34°C.

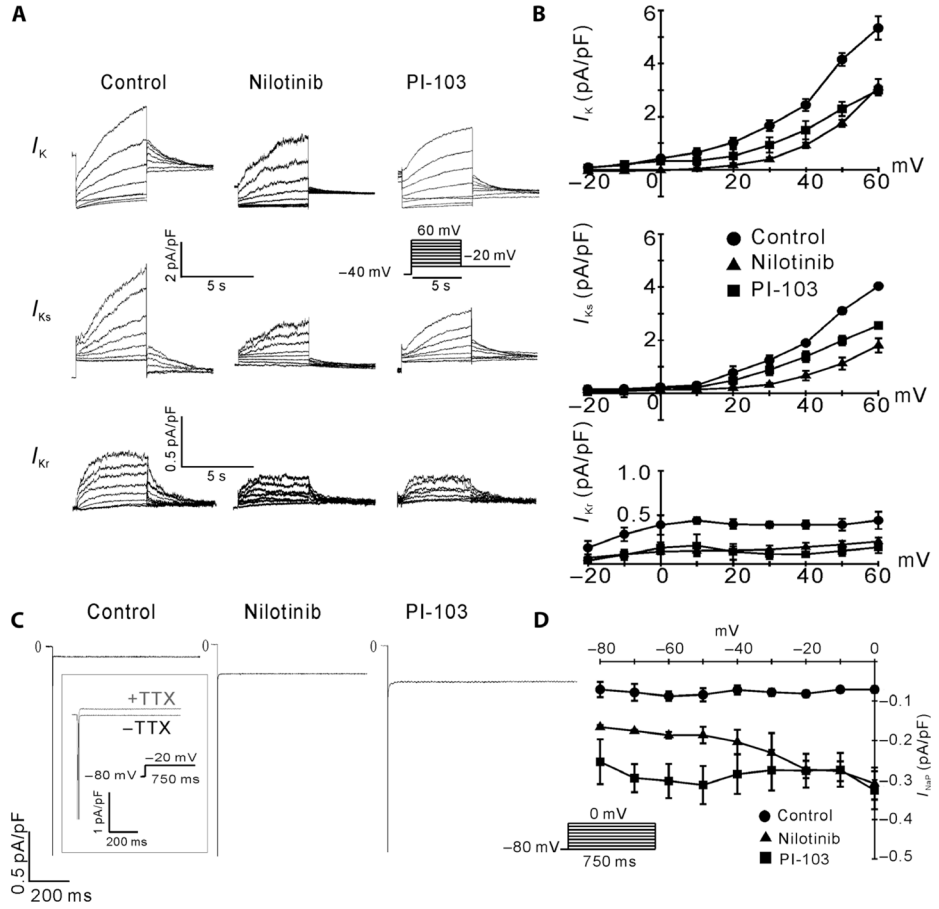

Fig. 3.

Effects of nilotinib and PI-103 on canine cardiac ion currents. (**A**) Sample traces of total outward rectifier current (I_K), chromanol 293B–sensitive component (I_{Ks}), and dofetilide-sensitive component (I_{Kr}) for canine myocytes treated with vehicle (control), 1 μM nilotinib, or 500 nM PI-103. (**B**) Leak-subtracted time-dependent *I-V* relationships of I_K, I_{Ks}, and I_{Kr}. $n = 5$ cells for each group. (**C**) Sample traces of tetrodotoxin (TTX)–sensitive I_{NaP} for myocytes treated with vehicle, 1 μM nilotinib, or 500 nM PI-103 in 50 mM external Na^+. TTX-sensitive currents were obtained by subtracting traces obtained in the presence of 10 μM TTX from the traces obtained in its absence (boxed traces). (**D**) *I-V* relationships of I_{NaP}. $n = 7$ cells for each group. The insets show the pulse protocols.

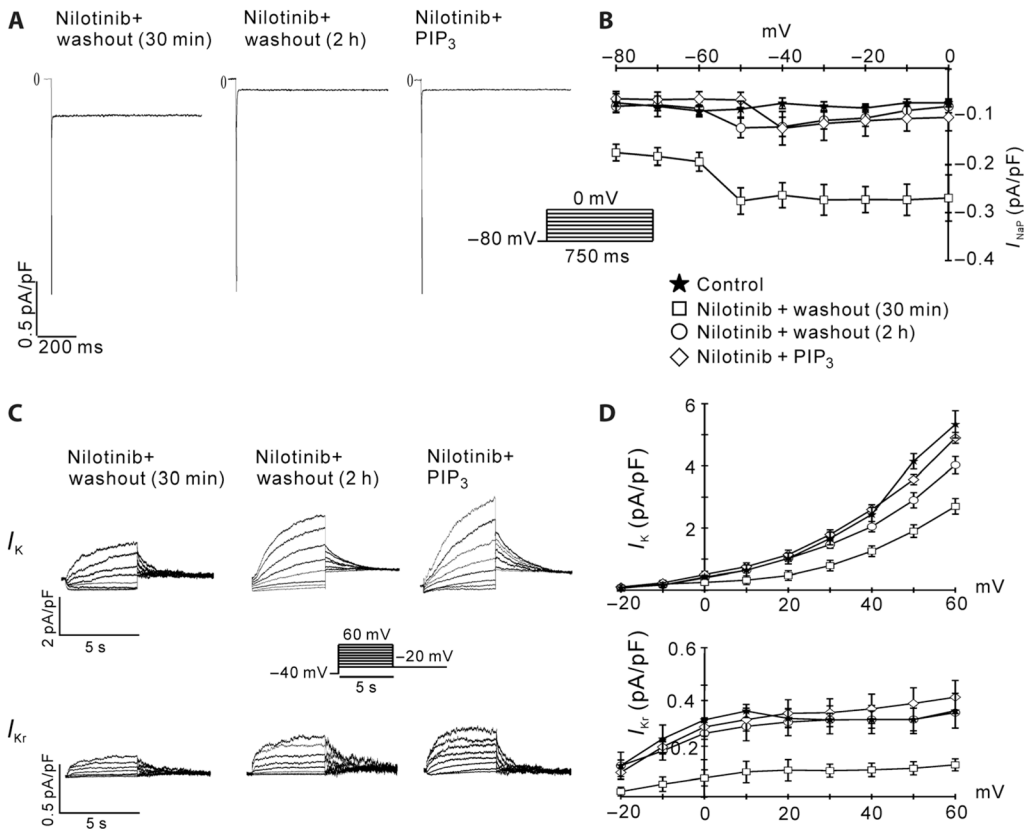

Fig. 4.

Reversal of nilotinib effects on I_{NaP} and I_{Kr}. Canine myocytes were treated with 1 μM nilotinib for 2 hours, and then the drug was washed out for either 30 min or 2 hours before patch clamping. In a separate experiment, cells were treated with nilotinib for 2 hours and then infused with 1 μM PIP_3 through the patch pipette. (**A**) Representative traces of I_{NaP} measured with 50 mM external Na^+. (**B**) *I-V* relationships of I_{NaP}. $n = 7$ cells for each condition. (**C**) Representative traces of I_K and I_{Kr}. (**D**) *I-V* relationships of I_K and I_{Kr}. $n = 6$ cells for each condition.

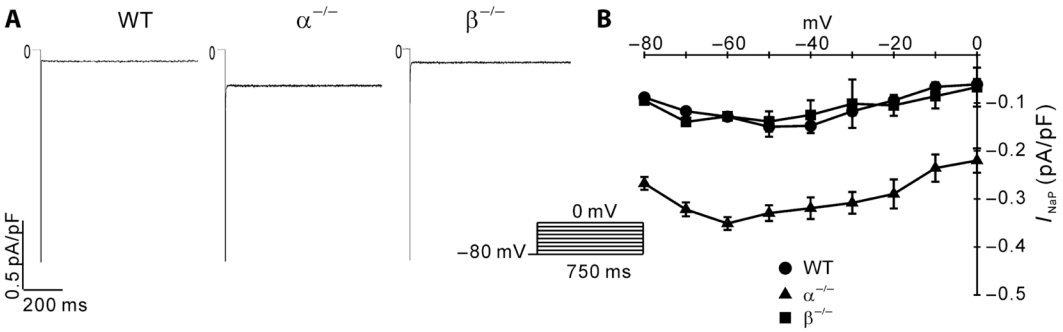

Fig. 5.

Effects of PI3K ablation on mouse I_{NaP} measured with 50 mM external Na^+. (**A**) Sample traces of TTX-sensitive I_{NaP} for wild-type (WT), $\alpha^{-/-}$, and $\beta^{-/-}$mouse myocytes. (**B**) *I-V* relationships for I_{NaP} in the three groups of mouse myocytes. The inset shows the pulse protocol for the activation of the Na^+ currents. $n = 7$ cells per group.

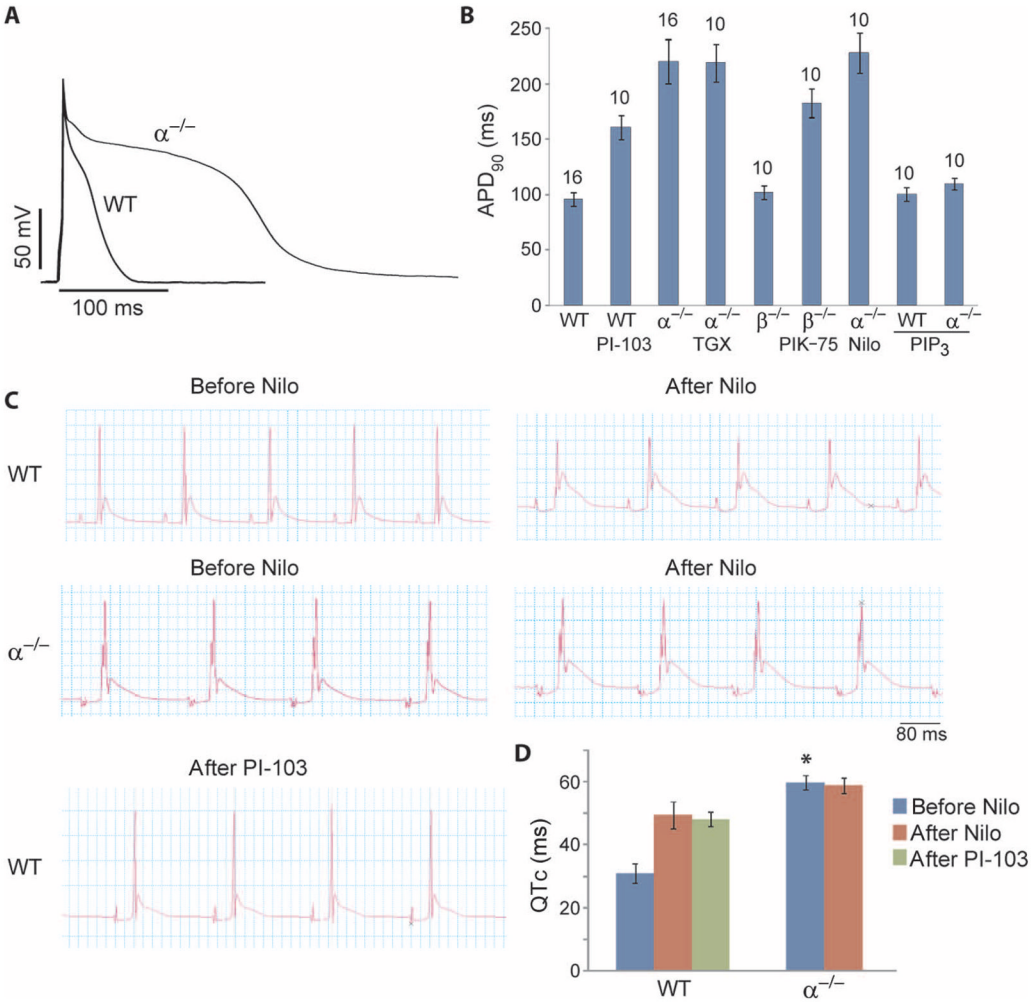

Fig. 6.

Effect of PI3K ablation on APD and the QT interval. APD_{90} was measured in the presence of 2 mM 4-AP. ECG recordings were obtained from spontaneously beating mouse hearts mounted on a Langendorff apparatus. (**A**) Representative action potentials recorded in cardiac myocytes isolated from $\alpha^{-/-}$ and WT mice. (**B**) Summary data of APD_{90} shown as means ± SE. The number of cells studied is above each bar. Where indicated, myocytes were incubated with 500 nM PI-103, 500 nM TGX-221, 100 nM PIK-75, or 1 μM nilotinib for 2 hours before measurements or dialyzed with 1 μM PIP_3 through the patch pipette. (**C**) Representative ECG tracings from $\alpha^{-/-}$ and WT hearts recorded before and after addition of 1 μM nilotinib or 1 μM PI-103 to the circulating bath. (**D**) Summary data of QT interval corrected for heart rate (QTc). Data are means ± SE. $n = 3$ hearts per group. $^*P < 0.05$, *t* test, significantly different from the WT before nilotinib group.

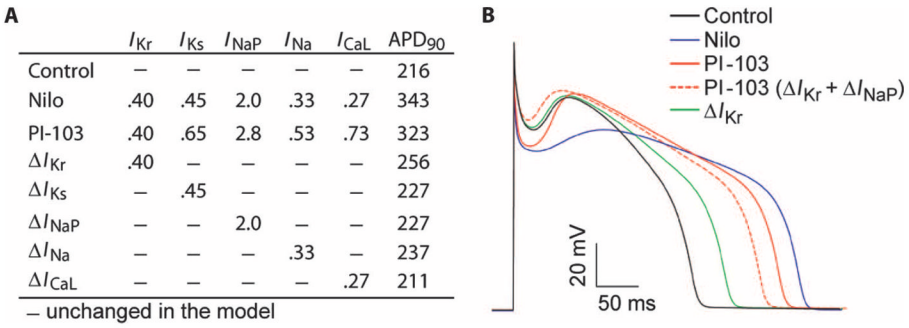

	I_{Kr}	I_{Ks}	I_{NaP}	I_{Na}	I_{CaL}	APD_{90}
Control	–	–	–	–	–	216
Nilo	.40	.45	2.0	.33	.27	343
PI-103	.40	.65	2.8	.53	.73	323
ΔI_{Kr}	.40	–	–	–	–	256
ΔI_{Ks}	–	.45	–	–	–	227
ΔI_{NaP}	–	–	2.0	–	–	227
ΔI_{Na}	–	–	–	.33	–	237
ΔI_{CaL}	–	–	–	–	.27	211

– unchanged in the model

Fig. 7.

Computer simulation of the effects of nilotinib and PI-103 on the canine ventricular action potential. (**A**) Ratio of ion current densities to control values based on experimental measurements (see Materials and Methods). Data for I_{Na} and I_{NaP} are from measurements in 10 mM external Na^+. Data for $I_{Ca,L}$ with PI-103 are from (19). (**B**) Simulations of the canine ventricular action potential using the modified Hund-Rudy model (see Materials and Methods). Control (black), nilotinib (blue), PI-103 (red), PI-103 effects on I_{Kr} and I_{NaP} only (dashed red), and ΔI_{Kr} (green).

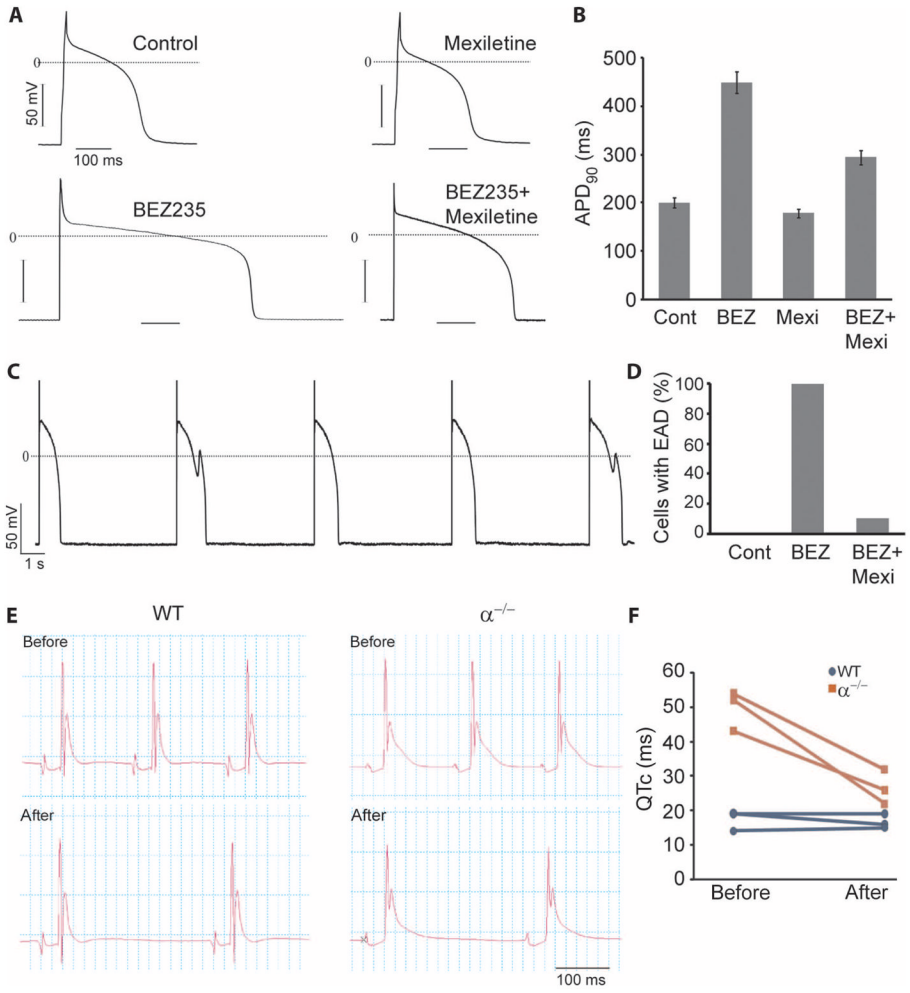

Fig. 8.

Reversal of APD and QT prolongation and EADs by mexiletine. (**A**) Representative action potentials recorded in canine myocytes treated with or without 500 nM BEZ235 in the presence or absence of mexiletine (4 μg/ml) for 2 hours. (**B**) Summary data of APD_{90} are shown in the graph. $n = 10$ cells for each group. (**C**) EADs induced by 5 μM ISO in BEZ235-treated myocytes. (**D**) Summary data of percentage of cells with EADs. $n = 10$ cells for each condition. (**E**) Representative ECG tracings from WT and p110α$^{-/-}$ (α$^{-/-}$) hearts before and after addition of mexiletine (4 μg/ml) to the circulating bath. (**F**) QT interval corrected for heart rate (QTc) from three hearts in each group.